Electron bombardment induced conductivity in amorphous silicon

Yoshinori Hatanaka, Hiroyasu Oi, and Takao Ando

Citation: Applied Physics Letters **39**, 637 (1981); doi: 10.1063/1.92837
View online: http://dx.doi.org/10.1063/1.92837
View Table of Contents: http://scitation.aip.org/content/aip/journal/apl/39/8?ver=pdfcov
Published by the AIP Publishing

Electron bombardment induced conductivity in amorphous silicon

Yoshinori Hatanaka, Hiroyasu Oi, and Takao Ando
Research Institute of Electronics, Shizuoka University 3-5-1 Johoku, Hamamatsu 432, Japan

(Received 12 May 1981; accepted for publication 4 August 1981)

The electron multiplication factors of electron bombardment induced conductivity (EBIC) of 300–500 were obtained with a hydrogenated amorphous silicon (*a*-Si:H) film of higher resistivity than 10^{10} Ω cm at an accelerating voltage of 7 kV. The response time of the EBIC current for a pulsed primary electron beam was determined to be shorter than 1 ms for both build-up and decay lags. It is found that an EBIC target of an *a*-Si:H film has promising properties for application to imaging devices at low light levels.

PACS numbers: 72.80.Ng, 79.90. + b, 85.60.Me, 85.10.Dt

Hydrogenated amorphous silicon (*a*-Si:H) has recently attracted much attention because of its low density of gap states, high photoconductivity, and a resistivity that exceeds 10^{10} Ω cm depending on the conditions of the deposition. This material is expected to be applicable to imaging devices such as vidicon type camera tubes[1,2] and electronic photographs.[3]

The electron bombardment induced conductivity (EBIC) effect was utilized for the image intensifier target of camera tubes for low light level use.The EBIC target using the materials such as As_2Se_3 (Ref. 4) PbO (Ref. 5), and ZnS (Ref. 6) have been investigated. However, the use of these materials for EBIC targets was not considered practically because of shortcomings such as image lag and after image. While the tube using single-crystalline silicon target, which is called an electronbombarded silicon (EBS) target tube[7,8] or a silicon intensified target (SIT) tube[9] have been utilized at low light levels, they have some disadvantages such as blooming caused by the excess carrier diffusion and low resolution limited by the diode array pitch.

In this letter, we report some experimental results of the EBIC effect in an *a*-Si:H film which are applicable to low light level imaging devices.

An inductively and capacitively coupled rf glow discharge deposition process was used to produce *a*-Si:H films from a 3% silane-hydrogen gas mixture. All the *a*-Si:H films were deposited at a pressure of 5 Torr and a substrate temperature of 200 °C. The cross-sectional configurations of the cells used in these experiments are shown in Fig. 1. Nondoped *a*-Si:H films were deposited 1 μm thick on the n^+ Si single-crystal wafer. In Fig. 1(a), a metal-thin insulator-amorphous silicon junction is constructed at the Al electrode side on the *a*-Si:H film, since that is expected to prevent carriers from being injected from the electrode and to decrease the dark current for imaging use. The thickness of the Al electrode and CeO_2 layers were 400 and 150 Å, respectively.

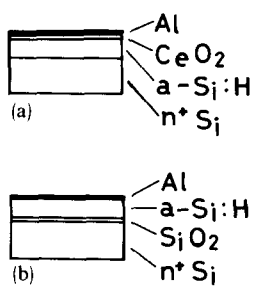

FIG 1. Configuration of cells used in experiment.

Figure 2 represents the *I-V* characteristics of the experimental cells. The axis of the abscissa represents the voltage applied to the Al electrode. As nondoped *a*-Si:H film is of *n* type, when a negative voltage is applied to the Al electrode in Fig. 1(a), the interface of the *a*-Si:H to CeO_2 is depleted and electron injection from the Al electrode is prevented as shown for curve (a) in Fig. 2.

Figure 3 shows the EBIC current characteristics measured as a function of the accelerating voltage of the primary electrons. The EBIC effect occurs at accelerating voltages above 2 kV, since an energy of 2 kV is needed for the penetration of Al-CeO_2 layers. The penetration depth of the accelerated electron can be evaluated to be less than 1 μm for the accelerating voltage of 8 kV from the single-crystal silicon data[7] and the energy loss in the Al-CeO_2 layers. The EBIC gain is defined as the ratio of the EBIC current to the primary electron current, and is seen to increase with the accelerating voltage. Typical value is 500 at an accelerating voltage of 7 kV. About the carrier generation for conduction, the gen-

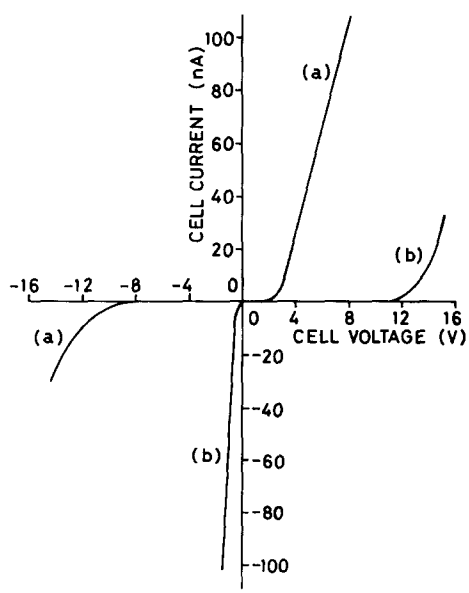

FIG. 2. *I-V* characteristics. Curve (a) is for (a) type cell in Fig 1, and curve (b) for (b) type cell.

 0003-6951/81/200637-03$00.50

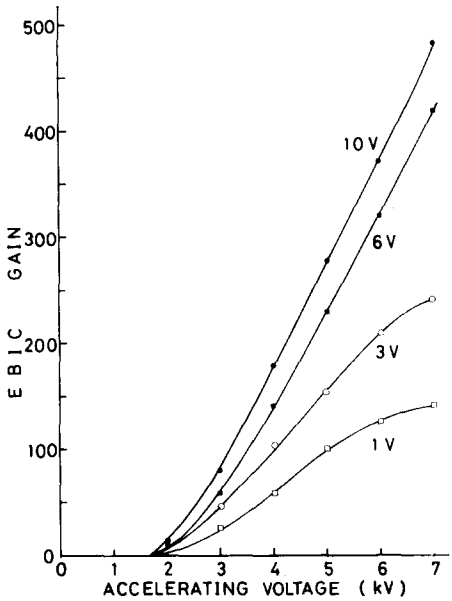

FIG. 3. Dependence of EBIC current on electron accelerating voltage. Parameters are cell voltages.

eration efficiency is expressed as follows:

$$\eta = \frac{G}{Va/Eg},$$

where G is the EBIC gain, Va the accelerating voltage, and

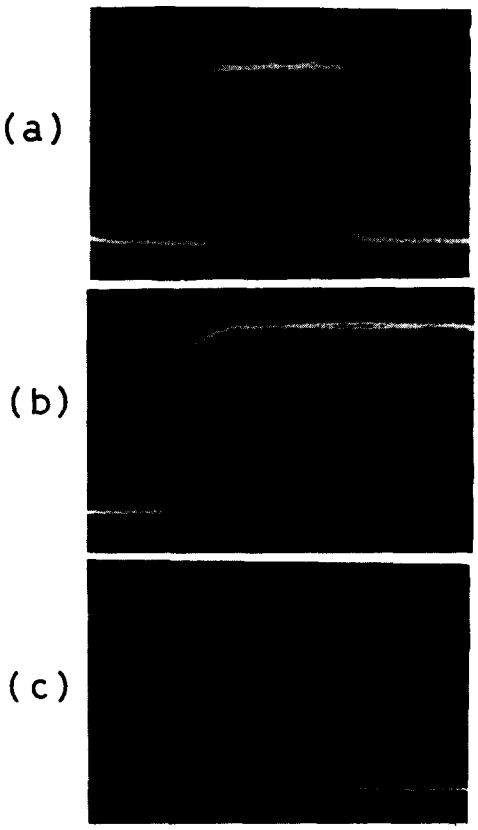

FIG. 4. Response wave form of EBIC current induced by a pulsive input current. Curve (a) is a typical wave form, and curves (b) and (c) are the enlarged illustrations of build-up and decay characteristics, respectively. Vertical: 100 nA/div. Horizontal: 5 ms/div. for curve (a), and 0.5 ms/div. for curves (b) and (c).

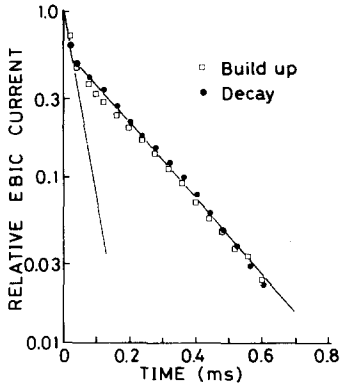

FIG. 5. Characteristics of the build-up and decay lags of the EBIC current.

Eg the mobility gap. For Va equals 7 kV, 5 kV, and 3 kV, G is 500, 280, and 80, and η is estimated to be 0.12, 0.09, and 0.04, respectively, under the assumption that $Eg = 1.7$ eV. Higher accelerating voltages gave rise to higher generation efficiency. It is considered for the reduction of η that at the low accelerating voltages, carrier recombination rate increases since carrier generation likely takes place near the interface between a-Si:H and CeO_2 and energy loss of primary electrons in the Al and CeO_2 layers plays a big role in the low accelerating voltages. At the low cell voltages in Fig. 3, the values of the generation efficiency are tended to reduce at high accelerating voltages. A large amount of carriers generated by the highly accelerated electrons is hard to be swept when the applied cell voltage is low, and space charge is expected to be generated in the a-Si:H layer. Therefore, the effective drift velocity of carriers seems to decrease and the efficiency is reduced. It is worthwhile to express that this space-charge effect is not observed except for the operating condition of very high accelerating voltage and low cell voltage.

Figure 4 shows pulsive responses of the EBIC current. It was measured for the following condition: the accelerating voltage of the primary electrons, primary electron current, cell voltage, and cell current were 5 kV, 2 nA, 8 V, and 500 nA, respectively. The resulting EBIC gain was 250. These time responses for both build-up and decay lags were plotted in semilogarithm chart as shown in Fig. 5. In this figure, the decay characteristics well fits to the build-up one. The presence of two relaxation processes is seen in this figure.

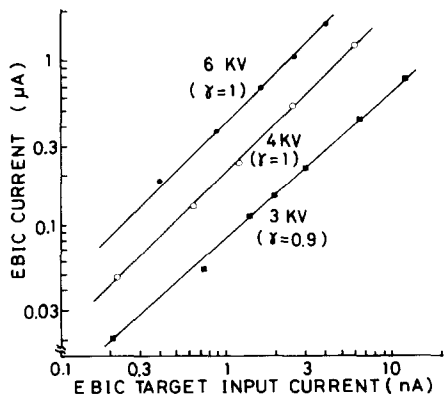

FIG. 6. γ characteristics: EBIC current vs primary electron current.

According to Loveland *et al.*,[10] free carrier lifetime in glow discharge *a*-Si:H is below 10^{-7} s. Time constant of the fast relaxation process in Fig. 5 is about 8×10^{-5} s, and is nearly the same as the time constant of the electric circuit used. Then the fast component may be considered as more fast relaxation process than the resulting value and to be caused by the free carrier lifetime. Time constant of the slow component is about 4×10^{-4} s. This component seems to involve a trap- limited process.

Figure 6 shows transfer characteristics of the EBIC current from the primary electron current, where the cell voltage was 10 V. Parameters in the figure are the accelerating voltages. When the EBIC current is defined to be proportional to γ power of the input current, γ values are nearly unity but decrease with decreasing the accelerating voltage. This may be due to the influence of recombination near the CeO_2-*a*-Si:H interface since carrier generation occurs near the interface in the low accelerating voltages. At sufficiently high cell voltages and high accelerating voltages, these EBIC currents are dominated mainly by monomolecular recombination since having the same relaxation time for both build-up and decay processes and having a unity γ value in the transfer characteristics.

In case of the cell shown in Fig. 1(b), the n^+ Si substrate acts as a metallic electrode, and this concentration is regarded as a metal-thin insulator-amorphous silicon junction. The SiO_2 layer was about 30 Å in thickness. The SiO_2 is expected to prevent the injection of electrons from the n^+ Si substrate. In case of the (b) type cell, EBIC gain was about 50–100, and was smaller than that of the (a) type cell. It is considered that in the (b) type cell, the charge carriers transported through the *a*-Si:H film are holes if the electron bombarded side was positively biassed against the silicon substrate and the electron-hole pairs are generated near the bombarded side. In case of (a), the transported carriers are electrons. The electron carrier type cell seems to give a larger EBIC gain than the hole carrier type cell. Therefore, since both electron and hole mobile carrier were shown in the experiments by using the two types of cells, space-charge effect is not appreciable in a *a*-Si:H film. This is consistent with the fact that the *a*-Si:H film does not have an after-image effect.

In summary, it was shown that the EBIC effect in an *a*-Si:H film yielded a gain of 300–500 and presented a fast-time response below 1 ms. It is also expected that the after-image effect of *a*-Si:H film is small since both electrons and holes are mobile carriers in this material. Consequently, we found that the EBIC effect in an *a*-Si:H film is applicable to image pick up devices, especially low light imaging devices, as this amorphous material has special characteristics such as antiblooming and high resolution.

The authors acknowledge the useful advice and encouragement received from Dr. R. Nishida, and the discussion on the amorphous silicon material from Professor S. Yamada and Dr. M. Kitao, and the discussion on the metal-thin insulator-silicon junction from Professor T. Yamamoto and Mr. K. Kawamura.

[1] Y. Imamura, S. Ataka, Y. Takasaki, T. Kusano, S. Ishioka, T. Hirai, and E. Maruyama, Proc. 11th Conf. Solid State Devices, Tokyo, Jpn. J. Appl. Phys. Supp. **19-1**, 573 (1980).
[2] I. Simizu, S. Oda, K. Saito, H. Tomita, and E. Inoue, in the Records of the Technical Meeting on the Electron Devices of the Inst. Elect. Comm. Eng. Jpn. **ED80-61**, 19 (1980).
[3] N. Yamamoto, Y. Nakayama, K. Wakita, M. Nikano, and T. Kawamura, Proc. 12th Conf. Solid State Devices, Tokyo, Jpn. J. Appl. Phys. Supp. **20-1**, 305 (1981).
[4] R. J. Schneeberger, G. Skorinko, D. D. Doughty, and W. A. Feibelman, Adv. Electron. Electron Phys. **16**, 235 (1962).
[5] P. H. Broerse, Adv. Electron. Electron Phys. **22A**, 323 (1966).
[6] D. R. Charles and M. Duchet, Adv. Electron. Electron Phys. **22A**, 305 (1966).
[7] S. Miyashiro, S. Shirouzu, S. Tsuji, and S. Horiuchi, Proc. IEEE **57**, 2080 (1969).
[8] D. Green, H. C. Nathanson, and G. W. Goetze, Paper presented at IEEE Int. Electron Devices Meeting, Oct. 1969.
[9] R. L. Rogers III, G. S. Griggs, W. N. Henry, P. W. Kaseman, R. E. Simon, and R. L. van Asselt, ISSCC Dig. Tech. Papers, 176 (1970).
[10] R. J. Loveland, W. E. Spear, and A. Al-Sharbaty, J. Non-Cryst. Solids **13**, 55 (1973/74).